SI-POF Supporting Power-Over-Fiber in Multi-Gbit/s Transmission for In-Home Networks

Fahad M. A. Al-Zubaidi ⓘ, *Student Member, IEEE*, David Sánchez Montero ⓘ, and Carmen Vázquez ⓘ, *Senior Member, IEEE*

Abstract—We propose the integration of power-over-fiber (PoF) in home networks with multi Gbit/s data transmission based on wavelength-division-multiplexing (WDM) in step-index plastic optical fibers (SI-POF). Different powering architectures are described. The efficiencies of different components are discussed to address the maximum remote energy that can be delivered. Experimental results show the ability of the system to deliver several mW of optical power with negligible data signal quality degradation and with BER of 1×10^{-10}. The potential of utilizing PoF in combination with low-loss WDM-POF to optically powering multiple devices for specific in-home applications and IoT ecosystems is discussed. A PoF scalability analysis is detailed.

Index Terms—Plastic optical fiber, home network, power-over-fiber, step index fiber, smart remote node, Internet of Things (IoT), sensor network.

I. INTRODUCTION

LARGE core step-index (SI) plastic optical fiber (POF) has been recognized as a strong candidate for in-home networking [1] due to many advantages such as easy installation and high bending tolerance in comparison with multimode silica fibers. Nowadays there is an increasing demand on operators to develop a home network that guarantees gigabit speeds to the customer due to the growth of different multimedia end-user services like high definition TV, IPTV or any Internet-based service [2]. Current home networks are predominantly a mixture of different network technologies, each originally optimized to carry a particular kind of communication service. Moreover, the booming amount of heterogeneous services supported by wireless devices may cause congestion in the radio-frequency (RF) spectrum as well as coverage and throughput issues thus hampering a reliable communication. Trends are becoming visible to make a transition to simplified pico- and/or femtocells which cover smaller areas suitable for the in-home scenario, generally

based on a single access point (AP) in each room, and thus reduce potential interference and congestion issues. Less transmitted power from antenna is then required but at the cost of requiring more APs. Another approach that is recently receiving growing attention is visible light communication (VLC) transmission, generally based on light emitting diodes (LEDs), which can be directly modulated and used as wireless transmitters [3]. Both approaches require a dedicated indoor fiber backbone network providing bandwidth enough to distribute the broadband signals to each wireless transmitter site, that may include wavelength-division-multiplexing (WDM) capabilities [4], [5]. And plastic optical fibers are one of the most promising candidates for the in-home distribution optical network.

Different bandwidth-efficient modulation schemes have been proposed to overcome the limited bandwidth of POF of around 200 MHz × 50 m, mainly due to intermodal dispersion, and to meet the expectation for the data rates required within the in-home scenario [6], [7]. Recently, many proposals report the capability of increased transmission capacity in terms of Multi Gbit/s, and particularly over SI-POF. 10 Gbit/s of data rate (R) over 10 m-long single SI-POF link with BER of 1×10^{-2} is achieved based on 32-PAM modulation and a multilayer perceptron-based equalizer utilizing a red laser diode (LD) [8]. POF large core diameter attract the use of light emitting diodes (LED) to achieve low cost links with the additional advantages of less eye damage risk for indoor free-space optics. In [9], 10 Gbit/s is achieved over 10 m with BER $< 1 \times 10^{-3}$ using two μLED and APD receivers. Violet, green and blue μLEDs are employed with PAM modulation in combination with WDM free-space components to achieve 11 Gbit/s over 10 m with BER $< 1 \times 10^{-3}$ [10]. In [11] a cyan LED with 47 μm active diameter is used with achieved data rates of 5.5 Gbit/s and 5.8 Gbit/s at BER of 1×10^{-3} over 1 m-long SI-POF with NRZ and 4-PAM modulations formats, respectively. The design of μLED-based arrays that can be used for VLC-POF links is also reported in [12]. Moreover, SI-POF links based on laser diodes with higher output powers and WDM technology are also proposed to extend the transmission distance up to 100 m with data rates of 10.7 Gbit/s and BER of 1×10^{-3} [13]. In [14] low-insertion loss multiplexer/demultiplexer devices are developed thus allowing the implementation of visible WDM links over SI-POF with low power penalty [14]. These Gbit/s communication speed experimental trials demonstrate the feasibility of using large core SI-POFs as the wired solution for indoor optical communication in the near future to meet end users' data rate demands.

On the other hand, Internet-of-Things (IoT) smart home applications can be easily integrated with the physical infrastructure of these in-home POF-based high capacity solutions. This technology is increasing rapidly everywhere including the in-home scenario and with different applications like healthcare, education and building architectures with the expectations of billion smart devices in the near future. IoT applications key aspects are ubiquity as well as energy demands of low-power, low-cost and small-sized smart remote nodes. The current evolution of low-power IoT ecosystems enables the utilization of Power-over-Fiber (PoF) systems to remotely feed sensor nodes via optical fiber [15]. PoF is of great advantage in environments with high electromagnetic interference (EMI) and provides inherent immunity to surrounding electromagnetic fields thus avoiding the use of any conventional EMI reduction technique for the power distribution. Step-index (SI) fibers are preferable over graded-index (GI) counterparts due to the mode field diameter restriction with respect to the maximum power injected into the fiber [16]. Some experiments over POFs reporting hundreds of mW of electrical power to the load have been demonstrated [17] and some partial analysis of the impact of PoF on SI-POF links have been discussed [18], [19]. Energy harvesting techniques from surrounding energy sources like heat and/or electromagnetism [20] can also be employed to generate additional electrical power supply in combination with PoF. Some proposals report energy harvesting systems based VLC that can provide electrical powers of around 1.5 mW [21], [22].

In this work, a real-time (RT) WDM system with maximum capacity of 4 Gbit/s over a 10 m-long SI-POF is proposed in combination with power-over-fiber (PoF) capabilities. The PoF system is implemented through the same POF fiber lead and shows the capability of providing energy to specific applications compatible with in-home wired/wireless IoT ecosystems. The potential of using PoF technology in these environments is also discussed. The system efficiency in terms of power per transmitted bit (P_{Tb}) for the data signal and the maximum energy that can be delivered by the PoF channel with no penalty in the data traffic quality is evaluated. A comparative study of our proposal with respect to current state-of-the-art for Multi Gbit/s systems over SI-POF is presented. Finally, a detailed study of the scalability of our proposed PoF system for remotely feeding a smart IoT ecosystem in the in-home scenario is addressed.

II. POWER OVER FIBER INTEGRATION IN INDOOR SOLUTIONS

A schematic of the integration of PoF for in-home networks is shown in Fig. 1. It considers the use of in-home SI-POF to provide gigabit per second communication as well as remote feeding purposes to the in-home IoT ecosystem. The integration of the PoF technology for powering smart remote IoT home nodes in the most efficient way is a major challenge in these future networks. The rapid growth in low-power integrated circuits allow the possibility of IoT devices with power consumption of few microwatts [23]. The consideration of the wired/wireless solution to connect these in-home IoT ecosystem is of great importance.
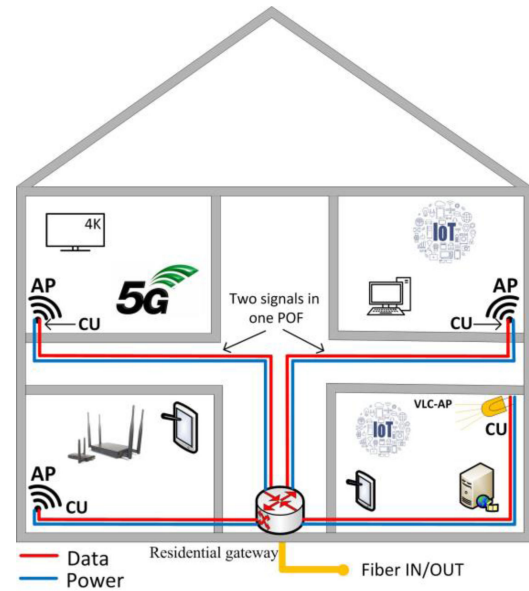

Fig. 1. Schematic of the proposed in-home network with PoF signal distribution.

Some aspects like maximum throughput and power consumption must be taken into account. Some technologies have been proposed to enhance the performance of wireless IoT systems in terms of energy saving by using different protocols with lower power consumption like LoRaWAN and low power WiFi [24], [25] compared to the current installed WiFi solutions. To connect the increased number of IoT devices current trends try to develop less power consumption devices but providing similar wireless connectivity. In [26] a new 28 μW ultra-low power consumption chip for wireless IoT connection is developed as a representative example. In this application scenario, we investigate the feasibility of PoF to provide energy for an in-home IoT ecosystem. A centralized PoF system is proposed compatible with most in-home network infrastructure approaches that have been proposed and investigated [1], [2], [27], where energy is delivered from the residential gateway to feed the entire IoT system from specific units named central units (CU). These CUs may be devoted for different indoor applications such as wireless access points or VLC communication purposes and may include different embedded smart functionality options.

The proposed system can integrate the future 5G indoor architectures where each room within the home can be equipped with high connectivity provided by POF, and simultaneously offering reliable optically feeding IoT solutions as shown in Fig. 1. Generally, the PoF system consists of a LD at the transmitter side to provide the power, the optical fiber link and a photovoltaic converter (PV) at the remote site/unit to convert the energy. The residential gateway can provide the energy to different elements. Different powering topologies can be designed to feed multiple battery-free smart nodes each of them with specific energy management systems for specific power consumption. Table I gives an example of main blocks of intelligent IoT nodes including smart sensors with power consumption in the μW range suitable for their use in IoT applications inside home.

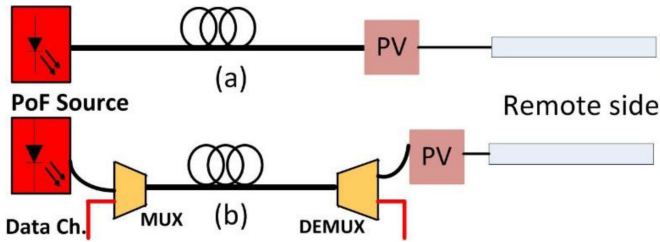| Function	Device	Type	Cons. (μW)
Control-intelligence	ECM3532	Artificial intelligence dual-core Arm Cortex-M3 plus NXP CoolFlux DSP	100
Communications	Ref. [26]	Wi-Fi connectivity	28
Monitoring-sensors	HTS221	Temperature and Humidity	7.2
	LPS33HW	Pressure	21.6
	H3lis331dl	Motion sensor	36
	ISM303DAC	Magnetometer sensor	17.1

Fig. 2. Different powering schemes. (a) Dedicated scenario. (b) Shared scenario. PV: Photovoltaic cell.

Using PoF can be cost-effective, achieving service continuity by remotely charging a node with local battery, and providing the ability of sending back information about link or device status as well as the measured information to the transmitter side in the case of a smart IoT home node. Moreover, this solution is compatible with potential energy harvesting capabilities embedded [28] in the node.

III. Power Over Fiber System Design

A. PoF Architectures

In any PoF system over data transmission media there are mainly two architectures: a shared fiber scenario by using the same fiber for simultaneous data transmission and PoF delivery, or a dedicated fiber scenario using two independent fibers for data and PoF, respectively, as shown in Fig. 2.

We can see that for the dedicated fiber scenario no optical DEMUX or filtering devices are needed at the reception stage, so the power can be directly delivered to the PV. However, these elements are required in the shared fiber scenario in order to split the data traffic in coexistence with the PoF signal into the same fiber lead. This fact leads to an extra penalty in the power delivery because of their insertion losses, but with the advantage of using a single fiber serving for both purposes. MUX devices are also needed to multiplex data and PoF in the shared scenario at the transmitter side.

MUX/DEMUX devices in such types of systems are critical as they should have acceptable insertion losses (IL) and high crosstalk (CT) with capability of handling high PoF power levels depending on the final application. The effect of these power levels on the data signal quality is of great importance.

B. Modeling Signal to Noise Ratio and Data Transmission Efficiency

When considering shared scenario, it is important to verify how PoF power levels can affect the data transmission quality and efficiency. As previously discussed for silica multicore fibers, with other requirements, in [29].

The optical signal to noise ratio (SNR) model when optically delivering different levels of power on the same optical fiber needs to consider the added signal at a different wavelength from the data signal counterpart. In our calculations, we consider two laser diodes, LD_1 for data transmission and LD_2 for the PoF channel. The optical power from LD_1 is P_1 providing a Relative Intensity Noise (RIN), shot noise limited, given by [30]:

$$\sigma_1 = \eta_{FO}\, P_1 \sqrt{RIN\, B} \tag{1}$$

$$\text{where}:\ RIN = \frac{2h\upsilon}{P_1} \tag{2}$$

where η_{FO} is the fiber attenuation, h is the Planck constant, υ is the optical frequency, and B is the bandwidth of the system.

The contributing noise terms at the detector with an incident optical power P_D, i.e. the shot noise (σ_2), dark current (I_D) noise (σ_3) and Johnson noise (σ_4), respectively, are given by:

$$\sigma_2 = \frac{1}{\eta_{PD}} \sqrt{2q\eta_{PD}P_D B} \tag{3}$$

$$\sigma_3 = \frac{1}{\eta_{PD}} \sqrt{2qI_D B} \tag{4}$$

$$\sigma_4 = \frac{1}{\eta_{PD}} \frac{1}{\eta_{Rx}} 2\sqrt{KT_A RB} \tag{5}$$

where η_{PD} is the conversion efficiency of the detector, q is the electric charge, K is Boltzmann constant, T_A is the temperature, η_{Rx}, is the preamplifier gain, and R is the resistance, respectively. R could be the feedback resistor value of a transimpedance amplifier, for example.

The SNR now can be expressed as follows:

$$SNR = \frac{P_D}{\sqrt{(\sigma_1)^2 + (\sigma_2)^2 + (\sigma_3)^2 + (\sigma_4)^2}} \tag{6}$$

The main difference is provided by the added term in σ_1 because of the RIN of the PoF laser; the effect will be higher for lower power levels of data channel at the receiver, P_D. By estimating the maximum power of PoF channel allowed at the receiver for a specific SNR we can determine the minimum crosstalk required at DEMUX device at reception, shown in Fig. 2.

About the data transmission efficiency, we define the power per transmitted bit (P_{Tb}) as [31]:

$$P_{Tb} = \frac{\beta \times I_{peak}}{T} \tag{7}$$

and

$$I_{peak} = m_i \times (I_{bias} - I_{th}) \tag{8}$$

where β is the quantum efficiency of the LD, m_i is the modulation index, and I_{bias} and I_{th} are the bias and threshold currents,
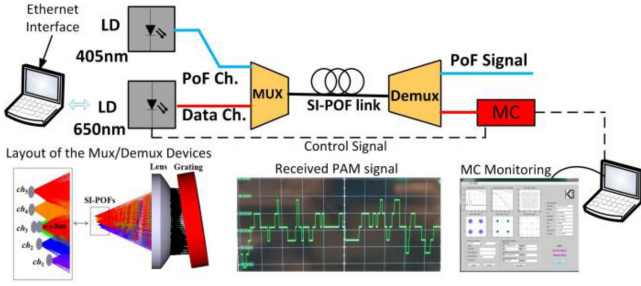
Fig. 3.   Schematic of the experimental setup.

respectively. T is the total network throughput and can be expressed as:

$$T = R^* [1 - \text{BER} (P_{\text{size}} + \text{IPG})] \tag{9}$$

where R^* is the data rate, P_{size} is the Ethernet packet size and IPG is the inter packet gap. By using these equations and depending on BER, the transmission efficiency yields:

$$\text{Transmission Efficiency} = \frac{T}{R^*} \times 100\% \tag{10}$$

Better BER values improve the transmission efficiency. For our experimental trials we select a system providing real Multi Gbit/s transmission in SI-POF [31] with BER of 10^{-10} for integrating PoF as well as testing impairment effects and energy efficiency degradation.

IV. Experimental Results

A. Experimental Testbed

In this work, we experimentally demonstrate Gbit/s data transmission with PoF in a shared scenario over SI-POF. The schematic of the experimental setup is shown in Fig. 3. It includes an optical SI-POF link, a power laser, a data transmitter and a receiver.

The set-up is based on a PC equipped with a 1 Gigabit Ethernet interface in combination with a Media Converter (MC) used to generate and to receive the transmitted data bits. The MC transforms the Gigabit Ethernet frames into a 16-level Pulse Amplitude Modulation (PAM) signal (named Tx-signal), and vice versa. At the transmitter side, the Tx-signal modulates the optical source of the data channel at 650 nm. The PoF signal is generated by a LD emitting at 405 nm. In this experiment, an external LD at 650 nm is used as the optical transmitter for the data channel instead of the LED provided by the MC in order to enhance the power budget of the link. Still the MC encodes the frames into a PAM signal and vice versa. Data and power channels are multiplexed and launched into a 10 m-long PMMA SI-POF link through a MUX device which is based on reflective diffraction grating technology with blazed profile and aspheric lens that can accommodate up to 6 channels with low insertion losses ILs ~ 4 dB, 3-dB bandwidth > 30 nm and size of ~ 65 mm x 55 mm. The designed MUX is bidirectional so another device with the same characteristics is used at the demultiplexing stage. Fig. 3 shows the layout of the MUX/DEMUX devices used,

however more details can be found in [14]. At the reception stage, the received optical signal is converted back to the electrical domain by a PIN photodiode (PD) included in the MC. This MC is part of a fully integrated system [32] that establishes a real-time data link at 1 Gbit/s without any post processing.

This system uses Multi-level Coset Codes (MLCC) for error correction and all the BER measurements in the next subsections are taken after the error correction process. The PD is monolithically integrated with the required amplifiers, logic and lenses. It features a high linear transimpedance amplifier for Gbit/s operation. The transmission system is chosen to have good performance in terms of high data capacity and BER to make it compatible with the application scenario discussed within Section II.

B. Measurements of PoF Impact on Data Transmission

In this section, the designed system is evaluated, including data signal quality and energy efficiency potential degradation due to PoF along with required devices specifications.

1) Shared Scenario and PoF Impact Analysis: To analyze if there is any influence in the data transmission quality when delivering different levels of power from the PoF signal on the same optical fiber we evaluate the evolution of the signal to noise ratio through the monitoring features provided by the MC. For doing so, different measurements of $\text{SNR}_{\text{decode}}$ (value detected by MC) and BER are carried out. All the measurements are done over a 10 m link length.

In the first set of measurements, there is no DEMUX in the reception stage to study the influence of the PoF signal (405 nm) into the data traffic channel (650 nm) so both signals reach the same PD. These measurements, apart from the impact effect on transmission, also provide data about the minimum CT specifications required at the DEMUX in the final application.

We use normalized measurements to evaluate the degradation. The reference signal is the measured $\text{SNR}_{\text{decode}}$ when the data signal is transmitted without PoF in the proposed setup. The measured $\text{SNR}_{\text{decode}}$ is 32.05 dB with a BER equals to zero. The PD accepts a maximum input power up to 0.5 dBm. For avoiding the damage of the PD, we config. the PoF power level at 405 nm received at the PD to be –0.2 dBm with additional received data signal of -8 dBm. In this case, the $\text{SNR}_{\text{decode}}$ degrades in 4.1 dB. We then decrease the optical power energy delivered in steps of 3 dB resulting in a $\text{SNR}_{\text{decode}}$ increment. This measured SNR shows negligible variations with respect to the reference signal up to a power channel level of $- 12$ dBm. In all the steps, the BER is $< 1 \times 10^{-10}$ that represents a free error transmission.

Afterwards, the input data signal is decreased, and set to -12 dBm and the PoF optical power delivered is set to -0.2 dBm, being both power levels measured at the PD. The same procedure to measure the $\text{SNR}_{\text{decode}}$ is done. The measured $\text{SNR}_{\text{decode}}$ is 28 dB when the data signal is transmitted alone. When both signals are multiplexed, the $\text{SNR}_{\text{decode}}$ decreases in 3.9 dB with PoF power channel at 405 nm of -0.2 dBm at the PD. The link is not established as the system requires $\text{SNR}_{\text{decode}} \geq 25$ dB for 1 Gbit/s transmission. The constellation
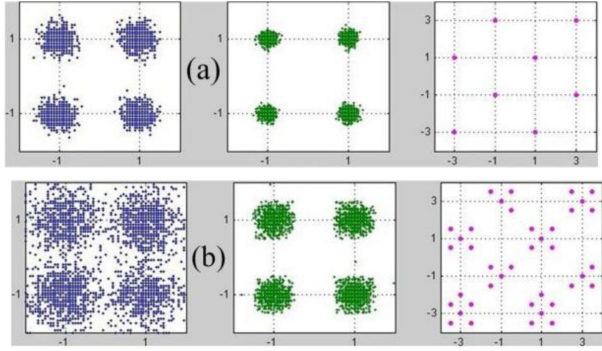
Fig. 4. Constellation diagram of the multilevel decoding inputs: (a) Only data signal, −8 dBm at PD. (b) Both data and PoF channels at PD; data −12 dBm, PoF − 0.2 dBm.

TABLE II
PARAMETERS FOR THE SNR ANALYSIS

Parameter	Value
η_{FO}, Total Att. of fiber	0.67
h, Plank constant	6.62×10^{-34} J.s
ν, frequency of the light	461.22 THz
B, Bandwidth of the system	500 MHz
η_{PD}, PD conversion efficiency	0.38 A/W
I_D, Dark current	10 nA
q, electric charge	1.6×10^{-19} C
K, Boltzmann constant	1.38×10^{-23} J/K
η_{Rx}, Preamplifier gain	1000 V/A
R, Resistance	1000 Ω
T_A, Temperature	300 K

diagrams of the three decoding stages at the receiver of the best and worst case are shown in Fig. 4. Using the equations (1) - (6) described within section 3. B, normalized SNR simulations are performed considering the parameters reported in Table II that are chosen to emulate our experimental setup.

We simulate two power levels reaching the PD, P_D of –8 dBm and −12 dBm in order to have a reference SNR value for no PoF signal injected into the link. As expected the SNR degrades as the power level impinging the PD decreases. Afterwards for simultaneous transmission, we add the noise contribution from the PoF channel (LD_2) to the overall noise power. RIN of the 405 nm channel affects the SNR of the data signal thus resulting in an additional penalty. Fig.5 shows a comparison between both normalized calculated SNR and measured SNR_{decode} which proves that they both have the same tendency against an increasing power from LD_2. Estimated SNR penalties are around 4-5 dB similar to that of observed from the experimental setup. We show that increasing the optical power delivery signal adds more noise to the system and both the SNR and BER degrade. The maximum
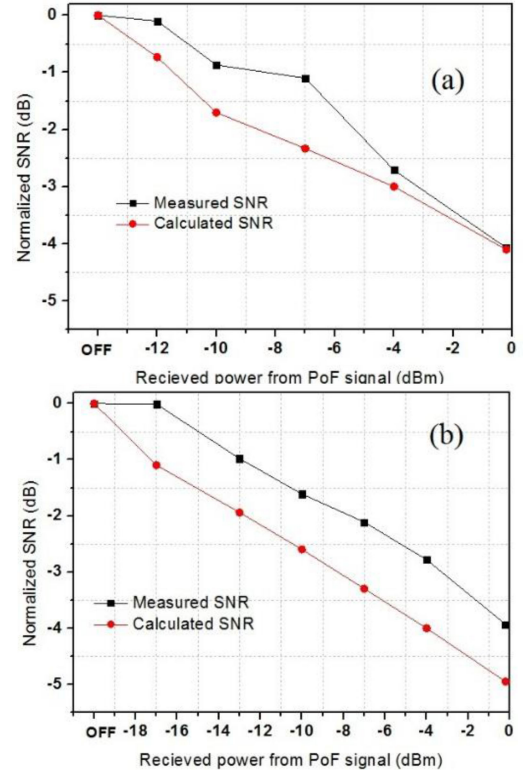

Fig. 5. Normalized calculated SNR and measured SNR_{decode} vs. PoF power at reception stage with input data signal power of: (a) −8 dBm (b) −12 dBm.

optical power of PoF at 405 nm, named P_{HPL}, that can reach the PD depends on the data signal power at 650 nm, named P_{DATA} reaching the PD.

In any case, from the experimental results, see Fig. 5, measured SNR curves, to keep the same SNR value as when there is no PoF, the relationship between the powers of both data and PoF channels at the PD can be expressed as:

$$P_{DATA}(dBm) - P_{HPL}(dBm) = 5\,dB \qquad (11)$$

The PoF power channel signal at MC PD, named $P_{HPL \cdot DEMUX}$, when using a DEMUX with a crosstalk CT at the reception stage yields:

$$P_{HPL\_DEMUX}(dBm) = P_{HPL}(dBm) - CT\,(dB) \qquad (12)$$

Then the required CT for the demultiplexer is given by:

$$CT = P_{HPL} - P_{HPL\_DEMUX} = P_{HPL} - P_{DATA} - 5\,dB \qquad (13)$$

As an example, for a 10 mW optical power delivery at the PV placed in the AP or VLC access point, see Fig 1, and receiving a data signal of −8 dBm a CT of 23 dB is then required.

2) Shared Scenario Including Demultiplexing and Data Transmission Performance: In order to recover the PoF signal and to study the received data signal, we use a DEMUX at the end of the link. This device uses a diffractive grating and have a CT of around 30 dB [14], complying with the requirements analyzed in the previous section. We evaluate the link performance using the monitoring features of the MC. The link is tested using different

TABLE III
POWER BUDGET OF THE PoF CHANNEL

Parameter	Power
LD output Power (dBm)	+13
Coupling loss (dB)	0.75
MUX/DEMUX IL (dB)	4
Link 10 m (dB)	2.1
Power at the end of link	+2.15 dBm or 1.64 mW

TABLE IV
RECENT PROPOSALS WITH 10M-LONG SI-POF LINKS

Parameter	This Work	[8]	[10]	[9]
Data Rate(Gbit/s)	$1^{(1)}$	10	11	10
BER	1×10^{-10}	1×10^{-2}	1×10^{-3}	1×10^{-3}
No. of Channels	$1^{(1)}$	1	3	2 bi
Simultaneous PoF	YES	NO	NO	NO
Real Time Trans.	YES	NO	NO	NO

Notes: (1) Can be extended up to 5 Gbit/s using 5 WDM-POF channels.

TABLE V
COMPARISON WITH RECENTLY REPORTED 10M-LONG SI-POF LINKS

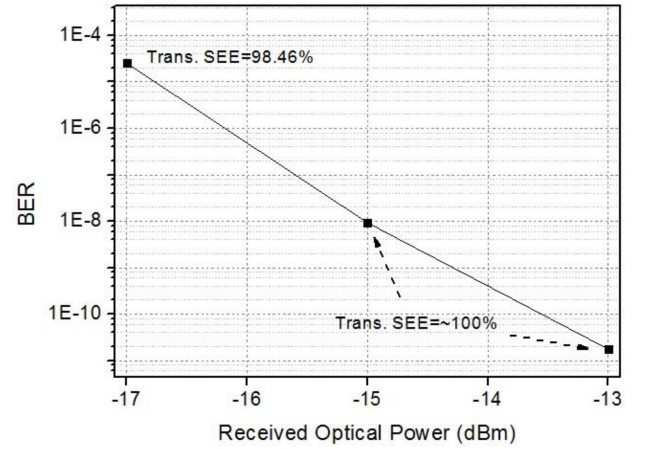| Parameter	This work 10 m	[8] 10 m	[13]100 m
Data Rate, R*(Gbit/s)	1	10	1.05
Wavelength (nm)	650	650	660
BER	1×10^{-10}	1×10^{-3}	1×10^{-3}
Data Throughput T (Gbit/s)	1	3.39	0.412
Transmission efficiency	1	0.339	0.392
Threshold Current I_{th} (mA)	20.4	20	80
Bias Current I_{bais}(mA)	23	30	45
Modulation index m_i	0.69	0.65	0.9
Quantum efficiency ß (W/A)	0.667	0.665	0.7-1.4
Power per bit P_{Tb} (pJ/b)	1.2	1.28	53.5

Fig. 6. Measured BER vs. received optical power with calculated transmission efficiency.

proposals on Multi Gbit/s transmission over 10 m-long SI-POF links. These calculations are done for the worst-case scenario considering 64 bytes of Ethernet packet size and IPG of 96 bits where only one bit-error results in a packet-error. Our system outperforms both previous works in terms of transmission efficiency and power per bit fig. s of merit, as described below.

We further investigate the performance of the system and analyze the impact of the BER on the total throughput and transmission efficiency. We vary the received optical power near the receiver sensitivity (~ -18.80 dBm) thus decreasing the BER. The results are shown in Fig. 6. For a received power greater than -13 dBm a BER of $< 1 \times 10^{-10}$ can be achieved with total throughput of 1 Gbit/s, meaning 100% of transmission efficiency. At BER of 1×10^{-5} the transmission efficiency is degraded to 98.46% thus leading to a throughput of 0.98 Gbit/s which still represents a good transmission performance. With the assumption of a further BER degradation to 1×10^{-3}, the transmission efficiency is 39%. These results show that the transmission efficiency of our system outperforms the other proposals at 10 m, with similar results to [31]. Moreover, a power per bit, P_{Tb}, of 1.2 pJ/b is achieved.

C. Discussion and Scalability Analysis

In this section, we discuss the use of PoF technology over the SI-POF link experimentally tested for feeding IoT nodes with the power consumption requirements provided in Table I. The central IoT unit/node has a control unit, WiFi communication capabilities as well as several sensors and demands around 150 μW. Other nodes have only communications and sensing capabilities demanding 30 μW.

The system energy efficiency (SEE) is a key issue in any PoF system. SEE depends directly on the optical to electrical conversion efficiency of the PV and the transmission efficiency of the fiber link. In general, SEE can be defined as follows:

$$\text{SEE} = \frac{\text{Energy at the remote node}}{\text{Energy of high power laser}} \quad (14)$$

Tx data power levels and varying the PoF optical power delivered at 405 nm. All the measurements are carried out in a 10 m-long SI-POF link. An estimation of the power budget of the PoF is shown in Table III. PoF power level of about 20 mW is injected into the fiber. BER measurements for different PoF levels show no impact of PoF on the data signal quality transmitted at 650 nm. In all cases, BER is $< 1 \times 10^{-10}$ that represents a free error transmission with the possibility of delivering 4.12 mW of optical power at the fiber end. The measured $\text{SNR}_{\text{decode}}$ of the link is 32 dB in both cases with no degradation due to the increments of the PoF signal level.

3) Shared Scenario Data Transmission Efficiency: In order to estimate the data transmission efficiency of the proposed setup, we analyze the power efficiency per transmitted bit based on the BER measurements. In our system with BER values of 10^{-10}, from Eq (9) and Eq. (10), we achieve a transmission efficiency of 100%. Table IV shows recent proposals of 10 m-long SI-POF links with their general parameters. Table V includes a detailed analysis of the transmission efficiency calculation of our proposed system compared to other current state-of-the-art
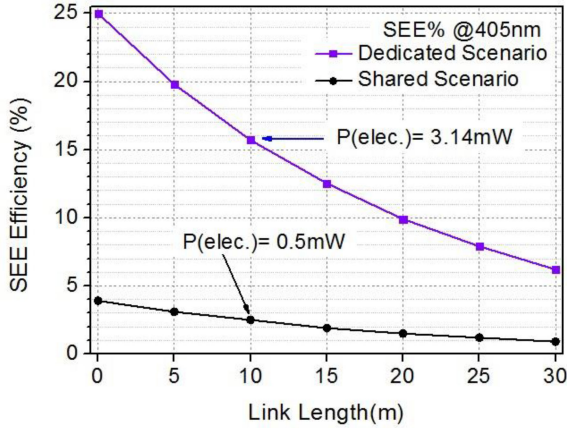
Fig. 7.   System energy efficiency (SEE) vs link length for the proposed experimental setup with MUX/DEMUX IL~4 dB, PV efficiency = 25%.

The SEE of the proposed system is analyzed considering the different powering architectures shown in Fig. 2, and depending on the PV efficiency (based on amorphous Silicon [33]), fiber attenuation and MUX/DEMUX losses. Wide bandgap materials with specific structure can be considered for higher quantum efficiency. The number of remote devices that can be powered via PoF provides information about how much the PoF solution is becoming reliable for a targeted application. For that we consider N as the number of remote nodes that can be optically feed to determine the scalability of the system. N directly depends on the power consumption on each remote node. For the calculation, we consider a simple node (N_A) that demands 30 μW and a central node (N_B) with additional embedded smart functionalities demanding 150 μW, respectively. Thus N_B the total number of central nodes that can be fed follows $N_B = N_A/5$.

From the power budget analysis described within Table III, after demultiplexing optical power up to 2 mW (reaching PV) for PoF signal is delivered for optimized HPL-POF fiber coupling loss. In Fig. 7, SEE of the proposed experimental setup is calculated for both shared and dedicated fiber scenario. The calculated electrical power at remote node (P_{elec}) is increased from 0.5 mW in the shared to 3.14 mW in the dedicated scenarios in the case of a 10m-long SI-POF link. As a result, and for this link distance, it yields $N_A = 16$ and $N_A = 104$ for the shared- and dedicated scenarios above described, respectively. Both node types could also be fed; for instance the shared scenario may lead to simultaneous $N_A = 6$ and $N_B = 2$ remote feeding.

Optimize ILs for the MUX/DEMUX devices can significantly enhance the SEE of the system thus increasing the resulting P_{elec} at the remote node. For that we analyze different cases as the fiber bundle approach proposed in [34] for POF multiplexing. This MUX is a fiber bundle made of graded index plastic optical fibers of 1m and NA of 0.185, having a total diameter of less than 1 mm; being faced with SI-POF using ST-ST connectors. At the DEMUX stage two cases are considered: our DEMUX device used for the experimental setup [14] as well as a potential improved version of the latter with extremely low losses (IL 1.5 dB). LD (PoF source) output power is considered to be
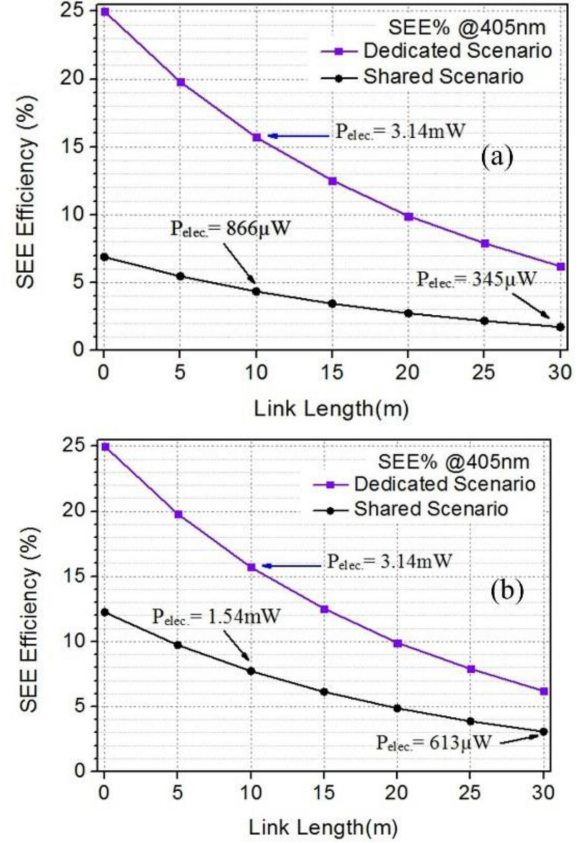

Fig. 8.   System energy efficiency (SEE) vs link length for the proposed experimental setup with fiber bundle for multiplexing, PV% = 25%:(a) DEMUX IL~4 dB, (b) DEMUX IL 1.5 dB
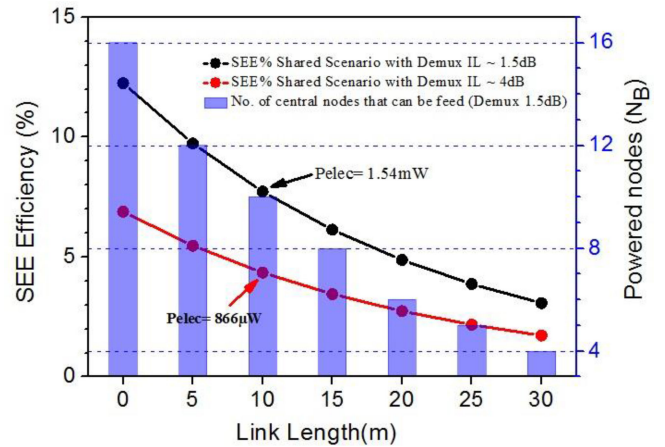

Fig. 9.   System energy efficiency (SEE) vs link length for the shared scenarios for PoF at 405 nm with different DEMUX losses. Right vertical axis: number of smart N_B IoT nodes that could be remotely fed considering different DEMUX devices in the link.

20 mW as aforementioned to fit with the experimental values. Fig. 8 shows the impact of consider this to the current experimental setup.

Fig. 9 shows a comparison between the two shared scenarios depicted in Fig. 8. SEE is increased from 4.1% to 8.9% for a 10
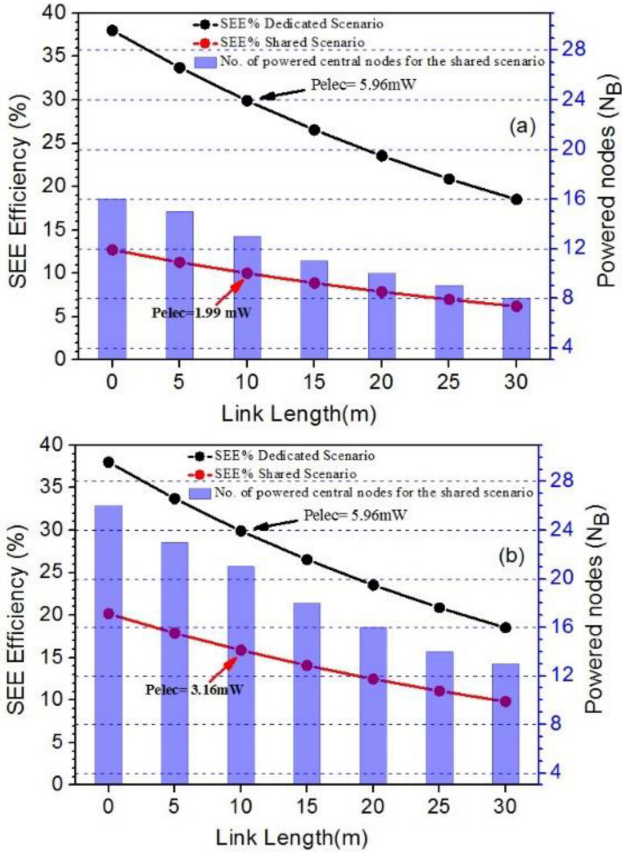
Fig. 10. System energy efficiency (SEE) vs link length for the proposed system considering a PoF system operating wavelength of 520 nm, LD output power: 20 mW, PV% = 38%, (a) DEMUX IL∼ 3.5 dB, (b) DEMUX IL 1.5 dB. Right vertical axis: number of smart N_B IoT nodes that could be remotely fed.

m-long link by using low loss proposed device. For this SI-POF link distance the remote delivered electrical power rises from 866 μW to 1.54 mW. This leads to an increase in the remote power delivery capability of the PoF system: N_A increases from 28 to 51 while the N_B counterpart from 5 to 10. Right vertical axis in Fig. 9 shows the evolution vs link distance of the smart N_B IoT nodes that could be remotely fed considering the case of a low insertion loss DEMUX device.

Other parameters that can affect the SEE should be considered like fiber attenuation and PV efficiency. Both depend on the operating wavelength of the PoF source. We consider a new wavelength for our study thus being 520 nm. At 520 nm both lower fiber attenuation coefficient (0.104 dB/m) and higher PV efficiency (∼ 38%) are expected compared to the 405 nm case.

Additionally, the DEMUX device shows a less insertion loss at this wavelength [14, 34] being of around 3.5 dB. In Fig. 10a, the SEE vs link length of the proposed setup with PoF at 520 nm is estimated for both shared- and dedicated- fiber scenario. At 10 m-long SI-POF link the remote electrical power delivered, P_{elec}, results in 1.99 mW and 5.96 mW for the shared- and dedicated scenarios. This means an increase of 129% and 90%, respectively, if we compare these values with the electrical power delivered, P_{elec}, at 10 m-long SI-POF, as shown in Fig. 8a. Fig 10b accordingly depicts the expected similar figures of merit by
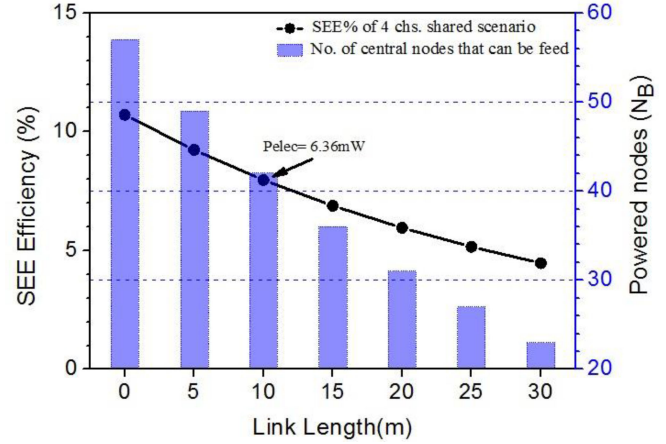

Fig. 11. System energy efficiency (SEE) vs link length for the proposed system considering 4 channels for PoF and one channel for data in a WDM-POF link for in-home networking.

considering the improved version of the DEMUX device with IL ∼1.5 dB. Following similar considerations to that of the previous figure, for this specific case study N_A increases from 66 to 105 while the N_B counterpart from 13 to 21, respectively.

Moreover, utilizing the presented MUX/DEMUX devices with high CT and acceptable ILs, the capacity of the proposed system can be extended to five channels. Data transmission of 4 Gbit/s can be integrated with the PoF levels concluded from Fig. s 7-10. On the other hand, the maximum delivered energy at the remote node can be even increased by applying more channels for optical feeding purposes.

Finally, in Fig. 11 we show the overall SEE vs link length for the shared scenario by using 4 channels for PoF (405 nm, 470 nm, 520 nm, 590 nm) and one channel for data (650 nm). The attenuation losses, MUX/DEMUX ILs for the rest of the channels are all extracted from [14], [31]. The delivered Pelec for a 10 m-long 5-channel WDM SI-POF link can be increased up to 6.36 mW. For this maximum energy delivery, $N_A = 212$ or $N_B = 42$ nodes could be remotely fed via PoF means which can be greatly enough for in-home scenarios.

For optical feeding based SI-POF (using the proposed channel at 405 nm), and depending on the power level, the long term stability of the fiber is of great importance. High temperature and humidity may cause aging problems as it can affect the optical properties of the fiber [35]. However, these problems can be expected in systems with high power levels increasing the fiber temperature up to 60° C [36], which is not the case in the proposed system using low power, being aging problems negligible. For high PoF system, this issue needs to be addressed. In [13], the same wavelength 405 nm is used in the data channel with the same power level we use.

The above analysis shows the feasibility of the designed PoF system to provide remote energy to multiple IoT devices with low power consumption. The numbers of optically feeding nodes can be increased by increasing the output power provided by PoF light source. Thanks to current state-of-the-art of low power consumption devices for IoT purposes provided in Table I, the

total PoF power can be reduced being able to operate in eye safety limit while providing sufficient energy to fulfill smart IoT ecosystem needs.

V. Conclusion

In this work we provide a detailed analysis of the impact of simultaneous data transmission and energy delivering over the same plastic optical fiber (POF) lead for the in-home networking scenario. A real-time data link at a data rate of 1 Gbit/s with BER $< 1 \times 10^{-10}$ over 10 m-long POF integrated with different energy delivery scenarios is evaluated. The transmission capacity of the proposed system can be expanded to 5 Gbit/s with the use of the presented MUX/DEMUX devices to achieve a WDM-POF based solution to expand the POF fiber data traffic capabilities and meet user's data rate demands in the home. Our system outperforms in terms of transmission efficiency and power per bit figures of merit.

We present shared and dedicated fiber scenarios over POF to integrate our PoF solution in the above POF communication link where no impact on the data traffic (BER $< 1 \times 10^{-10}$), neither on transmission efficiency is noticed for delivered optical power levels up to several mW at the fiber end. Design rules on the required crosstalk on the demultiplexer at the receiver stage are also provided. The use of this energy to remotely feed different sensor nodes for in-home IoT applications is discussed. The scalability of the system is analyzed showing the PoF feeding capabilities for different case studies that fulfill smart IoT in-home ecosystem needs.

References

[1] A. M. J. Koonen and E. Tangdiongga, "Photonics home area network," *J. Lightw. Technol.*, vol. 32, no. 4, pp. 591–604, 2014.

[2] Y. Shi *et al.*, "Plastic-optical-fiber-based in-home optical networks," *IEEE Comm. Mag.*, vol. 52, no. 6, pp. 186–193, Jun. 2014.

[3] I. N. Osahon, E. Pikasis, S. Rajbhandari, and W. O. Popoola, "Hybrid POF/VLC link with M-PAM and MLP equaliser," in *Proc. IEEE Int. Conf. Commun. (ICC)*, 2017, pp. 1–6.

[4] C. Lethien *et al.*, "Energy-autonomous picocell remote antenna unit for radio-over-fiber system using the multiservices concept," *IEEE Photon. Technol. Lett.*, vol. 36, no. 8, pp. 649–651, Apr. 2012.

[5] C. R. B. Correa, F. M. Huijskens, E. Tangdiongga, and A. M. J. Koonen, "POF feeding in Li-Fi systems with MIMO approach'," in *Proc. 24th annu. IEEE Photon. Benelux Symp.*, Amsterdam, Netherlands, 2019, pp. 1–4.

[6] B. Huiszoon, M. M. de Laat, Y. Shi, B. Eman, and G. N. van den Hoven, "Beyond a Gigabit on plastic optical fibre at the FTTH gateway," in *Proc. 15th Int. Conf. Trans. Opt. Netw. (ICTON)*, Cartagena, 2013, pp. 1–4.

[7] D. Fujimoto, H. Lu, K. Kumamoto, S. Tsai, Q. Huang, and J. Xie, "Phase-modulated hybrid high-speed internet/WiFi/Pre-5G In-building networks over SMF and PCF with GI-POF/IVLLC transport," *IEEE Access*, vol. 7, pp. 90620–90629, 2019.

[8] I. N. Osahon, M. Safari, and W. O. Popoola, "10-Gbit/s transmission over 10-m SI-POF with M-PAM and multilayer perceptron equalizer," *IEEE Photon. Technol. Lett.*, vol. 30, no. 10, pp. 911–914, 2018.

[9] X. Li *et al.*, "Micro-LED-based single-wavelength bi-directional POF link with 10 Gbit/s aggregate data rate," *J. Lightw. Technol*, vol. 33, no. 17, pp. 3571–3576, 2015.

[10] X. Li *et al.*, "11 Gbit/s WDM transmission over SI-POF using violet, blue and green μLEDs," in *Proc. Opt. Fiber Commun. Conf. (OFC)*, California, 2016, Paper Tu2C.5.

[11] J. Vinogradov *et al.*, "GaN-based cyan light-emitting diode with up to 1-Ghz bandwidth for high-speed transmission over SI-POF," *IEEE Photon. J.*, vol. 9, pp. 1–7, Jun. 2017.

[12] J. F. C. Carreira, "On-chip GaN-based dual-color micro-LED arrays and their application in visible light communication," *Opt. Express*, vol. 27, no. 20, pp. 1517–1528, 2019.

[13] R. Kruglov *et al.*, "10.7 Gbit/s WDM transmission over 100-m SI-POF with discrete multitone," in *Proc. Opt. Fiber Commun. Conf. (OFC)*, 2016, pp. 1–3.

[14] P. Pinzón, I. Pérez, and C. Vázquez, "Efficient multiplexer/demultiplexer for visible WDM transmission over SI-POF technology," *J. Lightw. Technol.*, vol. 33, no. 17, pp. 3711–3718, 2015.

[15] J. D. López-Cardona, D. S. Montero, and C. Vázquez, "Smart remote nodes fed by power over fiber in internet of things applications," *IEEE Sens. J.*, vol. 19, no. 17, pp. 7328–7334, Sep. 2019.

[16] J. D. López-Cardona, C. Vázquez, D. S. Montero, and P. Contreras, "Remote optical powering using fiber optics in hazardous environments," *J. Lightw. Technol.*, vol. 36, no. 3, pp. 748–754, 2018.

[17] C. Vázquez *et al.*, "Integration of power over fiber on RoF systems in different scenarios," in *Proc. of SPIE 10128*, Broadband Access Communication Technologies XI, 101280E, Jan. 28, 2017, doi: 10.1117/12.2254805.

[18] M. A. Fahad Al-Zubaidi, D. S. Montero, C. Vázquez, and P. J. Pinzón, "Noise analysis and Multi-Gbit/s transmission in PoF scenarios over SI-POF," in *Proc. XI Spanish Optoelectron. Meeting*, Zaragoza, Spain, 2019, Paper SP3.COM07.

[19] Fahad M. A. Al-Zubaidi, D. S. Montero, A. Lopez, J. Zubia, and C. Vázquez, "Investigation of power over fiber impact on gigabit data transmission in SI-POF," in *Proc. Int. Conf. Plastic Opt. Fiber*, Yokohama, Japan, 2019, pp. 45–46.

[20] V. Sharma, U. Mukherji, V. Joseph, and S. Gupta, "Optimal energy management policies for energy harvesting sensor nodes," *IEEE Trans. Wireless Commun.*, vol. 9, no. 4, pp. 1326–1336, Apr. 2010.

[21] X. Liu, X. Wei, L. Guo, Y. Liu, Q. Song, and A. Jamalipour, "Turning the signal interference into benefits: Towards indoor self-powered visible light communication for IoT devices in industrial radio-hostile environments," *IEEE Access*, vol. 7, pp. 24978–24989, 2019.

[22] G. Pan, J. Ye, and Z. Ding, "Secure hybrid VLC-RF systems with light energy harvesting," *IEEE Trans. Commun.*, vol. 65, no. 10, pp. 4348–4359, Oct. 2017.

[23] D. Tokmakov, S. Asenov, and S. Dimitrov, "Research and development of ultra-low power LoraWan sensor node," in *Proc. IEEE XXVIII Int. Scientific Conf. Electron. (ET)*, Sozopol, Bulgaria, 2019, pp. 1–4.

[24] J. Lee, Y. Su, and C. Shen, "A comparative study of wireless protocols: Bluetooth, UWB, ZigBee, and Wi-Fi," in *Proc. 33rd Annu. Conf. IEEE Ind. Electron. Soc. (IECON)*, Taipei, Nov. 2007, pp. 46–51.

[25] A. Nikoukar, S. Raza, A. Poole, M. Güneş, and B. Dezfouli, "Low-power wireless for the Internet of Things: Standards and applications," *IEEE Access*, vol. 6, pp. 67893–67926, 2018.

[26] P. Wang, C. Zhang, H. Yang, D. Bharadia, and P. Mercier, "A 28 μW IoT Tag that can communicate with commodity WiFi transceivers via a single-side-band QPSK backscatter communication technique," in *Proc. of ISSCC Conf.*, San Francisco, Feb. 2020, pp. 312–313.

[27] F. Forni, Y. Shi, N. C. Tran, H. P. A. van den Boom, E. Tangdiongga, and A. M. J. Koonen, "Multiformat wired and wireless signals over large-core plastic fibers for in-home network," *J. Lightw. Technol.*, vol. 36, no. 16, pp. 3444–3452, Aug. 2018.

[28] S. Mondal and R. Paily, "On-chip photovoltaic power harvesting system with low-overhead adaptive MPPT for IoT nodes," *IEEE Internet of Things J.*, vol. 4, no. 5, pp. 1624–1633, Oct. 2017.

[29] C. Vázquez *et al.*, "Multicore fiber scenarios supporting power over fiber in radio over fiber systems," *IEEE Access*, vol. 7, pp. 158409–158418, 2019.

[30] R. Dahlgren, "Noise in fiber optic communication links," *Tech. Rep., SVPhoton.*, 2000. [Online]. Available: http://www.svphotonics.com/pub/pub029.pdf

[31] P. J. Pinzón, I. Pérez, and C. Vázquez, "Visible WDM system for real time multi-gbit/s bidirectional transmission over 50m SI-POF," *IEEE Photon. Technol. Lett.*, vol. 28, no. 15, pp. 1696–1699, 2015.

[32] Knowledge Development for POF (KDPOF). "Simple introduction to gigabit communications over POF", 2014. [Online]. Available: http://www.kdpof.com/wp-content/uploads/2012/07/Easy-Introduction-v1.1.pdf, Accessed on: 15 Jan. 2016.

[33] E. J. H. Skjølstrup and T. Søndergaard, "Design and optimization of spectral beamsplitter for hybrid thermoelectric-photovoltaic concentrated solar energy devices," *Sol. Energy*, vol. 139, pp. 149–156, 2016.

[34] P. J. Pinzón, J. Moreno, and C. Vázquez, "Energy efficiency of a WDM link at Multi-Gbit/s over plastic optical fiber," in *Proc. of XXXI Nat. Symp. Int. Scientific Radio Union (URSI)*, Madrid, 2016, pp. 1–4.

[35] K. Bhowmik and Gang-Ding Peng, "Polymer Optical Fiber" book chapter, Handbook of Optical Fibers, Springer Nature Singapore, pp. 1–51, Mar. 2019, doi: 10.1007/978-981-10-1477-2_38-1.

[36] A. D. Alobaidani, D. Furniss, M. S. Johnson, A. Endruweit, and A.B. Seddon, "Optical transmission of PMMA optical fibres exposed to high intensity UVA and visible blue light," *Opt. Laser Eng.*, vol. 48, pp. 575–582, 2010.

Fahad M. A. Al-Zubaidi (Student Member, IEEE) received the M.Sc. degree in laser/electronic and communication engineering from the University of Baghdad, Baghdad, Iraq, in 2015. He is currently working toward the Ph.D. degree in electrical, electronics and automation engineering with UC3M, Leganés, Spain. He was awarded research scholarship to join the Huazhong University of Science and Technology, China, during his master's studies. His research interests include plastic optical fibers, 5G cellular networks, radio over fiber, and power over fiber systems.

David Sánchez Montero received the Ph.D. degree from the Department of Electronics Technology, UC3M, Leganés, Spain, in 2011. He is currently an Associate Professor with the Department of Electronics Technology, UC3M. His current research interests are focused on fiber-optic sensors, multicore optical fibers, WDM-PON networks, and power over fiber systems. He is currently involved within the H2020 Bluespace project.

Carmen Vázquez (Senior Member, IEEE) received the M.Sc. degree in physics (Electronics) from the Complutense University of Madrid, Madrid, Spain, in 1991, and the Ph.D. degree in photonics from the Telecommunications Engineering School, Polytechnic University of Madrid, Madrid, Spain, in 1995. She received a Fellowship with TELECOM, Denmark, in 1991,working on erbium-doped fiber amplifiers. From 1992 to 1995, she worked with the Optoelectronics Division, Telefónica Investigación y Desarrollo. She was involved in III.V integrated optics devices characterization, design, and fabrication. In 1995, she joined the Carlos III University of Madrid, Getafe, Spain, where she is currently a Full Professor with the Department of Electronics Technology and the Head of the Displays and Photonic Applications Group. She was a Visiting Scientist with the Research Laboratory of Electronics, Massachusetts Institute of Technology, from 2012 to 2013, working on silicon photonics. She was also the Head of the Department for three years and the Vice-Chancellor for four years. Her research interests include integrated optics, optical communications and instrumentation, including, plastic optical fibers, broadband access networks and monitoring techniques, RoF systems, filters, switches, fiber optic sensors, and WDM networks. She is the coauthor of more than 200 scientific publications and is the holder of six patents. She has participated in different European projects and networks in the ESPRIT, RACE, and IST framework programs, such as PLANET, OMAN, HEMIND, SAMPA, EPhoton/One+, BONE, BlueSpace (*Building on the Use of Spatial Multiplexing 5G Networks Infrastructures and Showcasing Advanced technologies and Networking Capabilities*), and has led several national researching projects and consortium, such as SINFOTON2-CM. She is a Fellow of the SPIE.